

Synthesis and low-temperature photoluminescence properties of SnO₂ nanowires and nanobelts

Suhua Luo^{1,2}, Jiyang Fan^{2,3}, Weili Liu¹, Miao Zhang¹,
Zhitang Song¹, Chenglu Lin¹, Xinglong Wu^{2,3} and
Paul K Chu^{2,4}

¹ Research Center of Semiconductor Functional Film Engineering Technology, Shanghai Institute of Microsystem and Information Technology, Chinese Academy of Sciences, Shanghai 200050, People's Republic of China

² Department of Physics and Materials Science, City University of Hong Kong, Tat Chee Avenue, Kowloon, Hong Kong, People's Republic of China

³ National Laboratory of Solid State Microstructures and Department of Physics, Nanjing University, Nanjing 210093, People's Republic of China

E-mail: paul.chu@cityu.edu.hk

Received 26 November 2005, in final form 1 February 2006

Published 27 February 2006

Online at stacks.iop.org/Nano/17/1695

Abstract

Ultra-long rutile tin dioxide nanowires and nanobelts are synthesized by thermal oxidation of tin powder using gold film as the catalyst. Nanowire or nanobelts can be selectively produced by tuning the reaction temperature. The vapour–liquid–solid growth mechanism is proposed. The band gaps of the nanowires and nanobelts are 3.74 and 3.81 eV respectively, determined from UV/visible absorption spectral results. The SnO₂ nanowires show stable photoluminescence with two emission peaks centred at around 470 and 560 nm. Their wavelengths stay almost fixed while their intensities depend sensitively on the temperatures within the examination ranges from 10 to 300 K. The SnO₂ nanobelts show similar photoluminescence behaviours and the origin of the luminescence is discussed.

1. Introduction

As an n-type wide band gap semiconductor ($E_g = 3.6$ eV at 300 K for bulk SnO₂), one-dimensional (1D) tin oxide nanostructures have attracted great interest in recent years. The nanostructures are particularly useful in gas sensors and optical devices due to their high surface to volume ratio, chemical stability, remarkable resistivity variation in a gaseous environment, and high exciton binding energy of 130 MeV. Much progress has been achieved in the synthesis and structural characterization of 1D SnO₂ nanostructures [1–5]. In addition, owing to their electrical and sensing properties [6–9], the use of the nanostructures in real devices is progressing rapidly [10–14]. However, some fundamental issues pertaining to the optical properties of 1D SnO₂ nanostructures are still unclear [15].

Optical measurements such as photoluminescence (PL) are very useful for the determination of the structure, defects, and impurities in these nanostructures, and there have been several reports on the luminescence of 1D SnO₂ nanostructures at room temperature [15–20] showing emission in the range 400–600 nm. The luminescence is generally believed to stem from defects such as tin interstitials, dangling bonds, or oxygen vacancies. However, direct proof that such defects are incorporated in the luminescence centre has not yet been given.

In the work reported here, we investigated the temperature dependence of the full PL spectrum from high-quality SnO₂ single-crystal nanowires and nanobelts as well as the structure and morphology of the nanostructures. A new luminescence band at 470 nm at a temperature lower than 100 K was found for the first time, and it showed a very strong dependence on the temperature. Our experimental results show that surface oxygen vacancies are the possible origin of the luminescence.

⁴ Author to whom any correspondence should be addressed.

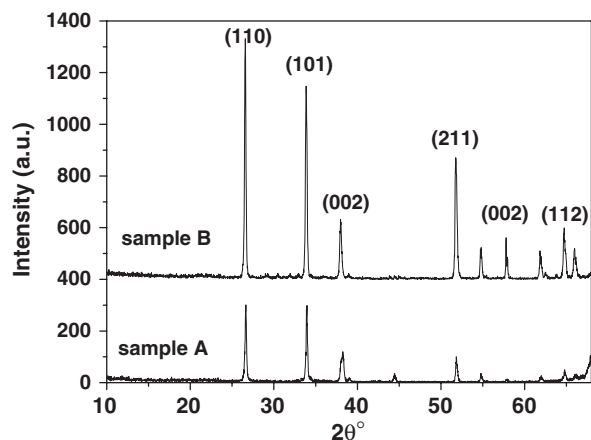


Figure 1. X-ray diffraction patterns of the synthesized SnO₂ nanowires (sample A) and nanobelts (sample B).

2. Experimental details

In our materials synthesis, a 100 cm long horizontal quartz tube with an inner diameter of 50 mm open on one side was mounted inside a high-temperature quartz tube furnace. 99.99% pure tin powders were placed in an alumina boat positioned at the centre of the quartz tube. A gold-coated (20 nm thick) p-type (100) Si wafer was used as the substrate. The temperature in the furnace was rapidly ramped up to 850 °C (sample A) or 1000 °C (sample B) and kept for 60 min. During the process, a constant flow of Ar (99.99%) at a rate of 50 sccm was maintained. After cooling to room temperature, white wool-like products were found on the substrate.

The morphology and crystal structure of the synthesized nanostructures were characterized by x-ray diffraction (XRD) using a D/max 2550V utilizing Cu K α radiation, scanning electron microscopy (SEM) employing a JSM-6700F, and high-resolution transmission electron microscopy (HRTEM) using a JEM200F. UV/visible absorption measurements were carried out on the SnO₂ nanowires and nanobelts using a spectrophotometer (U-2000, Hitachi) in a range between 200 and 2000 nm. The PL spectra at different temperatures were acquired from 340 to 640 nm using a 325 nm He–Cd laser.

3. Results and discussion

The structure and phase of the two samples as revealed by XRD are depicted in figure 1. Both samples possess the same structure that can be indexed to a pure rutile phase SnO₂ with lattice constants of $a = 4.738 \text{ \AA}$ and $c = 3.189 \text{ \AA}$. Figures 2(a) and (b) show typical SEM images of the samples. A large number of nanowires can be observed in sample A as shown in figure 2(a). These ultra-long SnO₂ nanowires have lengths of several hundred micrometres and appear to grow randomly on the Si substrate. The inset in figure 2(a) displays the magnified SEM image of a typical SnO₂ nanowire with a diameter of about 300 nm. The polyhedron particle located on the nanowire tip is identified to be Au by electron diffraction spectroscopy (EDS), indicating vapour–liquid–solid (VLS) growth of the nanowires [21]. The spherical droplets at the tips of the nanowires are commonly considered to be evidence

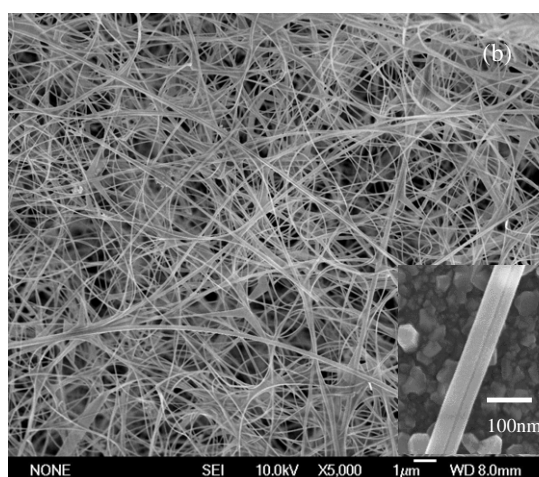
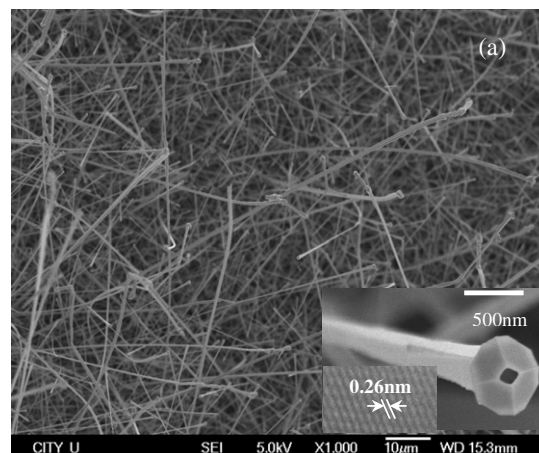


Figure 2. (a) SEM image of SnO₂ nanowires. The inset shows the higher-magnification image of a nanowire and the HRTEM image of a single nanowire. (b) SEM image of SnO₂ nanobelts. The inset shows the magnified image of a single SnO₂ nanobelt.

of the VLS mechanism. In this mechanism, Au and Sn form a liquid alloy droplet at a relatively low freezing temperature and it becomes the preferred site for deposition from the vapour. The HRTEM image displayed in the inset of figure 2(a) shows that this particular nanowire is a structurally uniform single crystal, and no dislocations or other planar defects exist. The inter-plane spacing of the selected nanowires is about 0.26 nm, which corresponds to the distance between the neighbouring (101) planes in the tetragonal rutile SnO₂ structure. Figure 2(b) shows the morphology of sample B. This sample also has a low-dimensional structural morphology and comparatively more even transverse size compared to sample A. One typical single nanobelt about 30 nm thick and 70 nm wide is shown in the inset of figure 2(b). No polyhedron particles can be found on the tips of the nanobelts, perhaps because of evaporation during the growth of the nanobelts. From the above results, nanowires can be produced under a low synthesizing temperature like 850 °C, whereas nanobelts are obtained at a higher temperature of 1000 °C. At an even higher synthesis temperature of about 1100 °C, nanostructures with more complicated morphologies are produced, but nanobelts still constitute the main products. Hence, we believe that

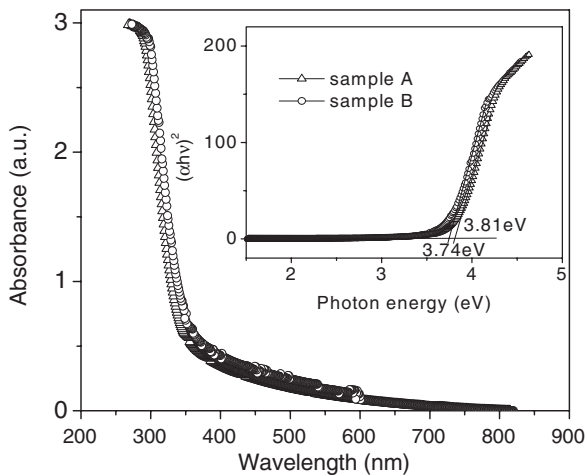


Figure 3. UV/visible absorption spectra of the SnO₂ nanowires and nanobelts. The inset shows the $(\alpha(h\nu))^2$ versus photon energy curve.

temperature plays an important role in the synthesis of nanostructures with different morphologies.

High-energy shift of an absorption edge is generally expected for nanocrystalline materials. In order to confirm this, absorption spectra were acquired from the SnO₂ nanowires and nanobelts, and the results are depicted in figure 3. The optical transition of SnO₂ crystals is known to be a direct type [22]. In this case, the absorption coefficient α is expressed as $\alpha(h\nu) \propto (h\nu - E_g)^{1/2}/h\nu$ [23]. Plots of $(\alpha(h\nu))^2$ versus $h\nu$ can be derived from the absorption data in figure 3. The intercept of the tangent to the plot gives a good approximation of the band gap energy of the direct band gap materials. This is ~ 3.74 eV for the nanowires and ~ 3.81 eV for the nanobelts, as shown in the inset of figure 3; both of which are larger than the value of 3.62 eV for bulk SnO₂ due to the quantum size effect [24, 25]. In addition, the larger band gap of the nanobelts than that of the nanowires also agrees well with their lower sizes as observed from SEM examinations.

The optical properties of a semiconductor are related to both intrinsic and extrinsic effects. PL is a suitable technique to determine the crystalline quality and the presence of impurities in the materials as well as exciton fine structures. The temperature dependence of the PL in the SnO₂ nanowires and nanobelts from 10 K to room temperature is shown in figures 4 and 5. In figure 4, the SnO₂ nanowires exhibit different luminescence bands at different temperatures, with 100 K serving as a transitional temperature. At temperatures lower than 100 K, the nanowires show an asymmetric, smooth, and broad luminescence band centred at around 470 nm (2.64 eV), while at higher temperatures, an asymmetric broad luminescence band centred at about 560 nm (2.21 eV) emerges. The transitional spectrum acquired at 100 K shown in the inset of figure 4 shows two deconvoluted subbands, one centred at 470 nm and the other at 560 nm. Therefore, there appear to be two types of emission centres in the nanowires. Further multiple-peak Gaussian fitting is applied to the whole collection of PL spectra for a given sample in order to study the temperature dependence of respective emission bands. The results show that the two different emission peaks all shift

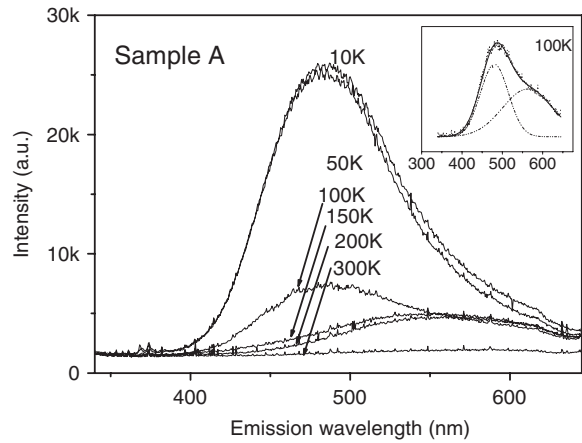


Figure 4. PL spectra of the SnO₂ nanowires acquired at different temperatures. The inset shows the multiple-peak Gaussian fit of the PL spectrum at 100 K.

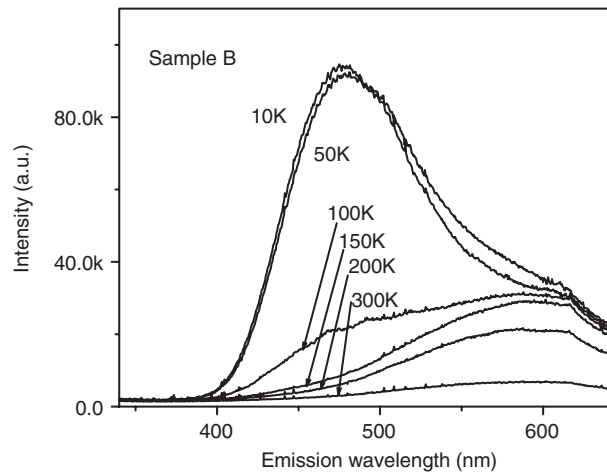


Figure 5. PL spectra of the SnO₂ nanobelts obtained at different temperatures.

slightly to lower energy with increasing temperature. The intensity of the emission peak centred at 470 nm decreases rapidly by about four times as the temperature rises from 10 to 100 K, and almost disappears at room temperature. The intensity of the peak centred at 560 nm decreases by about two times from 10 to 100 K and it dominates the luminescence at room temperature. Hence, the temperature has a much larger influence on the intensity of the emission band at 470 nm.

Since the band gap of the present SnO₂ nanowire is 3.74 eV (331 nm) as determined from the UV/visible absorption spectrum, the two observed luminescence bands cannot be ascribed to the direct recombination of a conduction electron in the Sn 4d band with a hole in the O 2p valence band. Broad luminescence bands between 400 and 600 nm have been reported from 1D SnO₂ nanostructures at room temperature [15–20]. The nature of the transition is generally believed to be Sn or O vacancies formed during the growth process inducing trapping states in the band gap. No detailed investigation has, however, been carried on the low-temperature PL properties of 1D SnO₂ nanostructures. Low-temperature PL in the range of 470–590 nm has been

reported from tin oxide powder and assigned to a single defect centre [26]. In contrast, our SnO₂ nanowires show two distinct emission peaks and different temperature dependence due to the two different luminescence defect centres in the SnO₂ nanowires. Moreover, the 470 nm peak may originate from a shallower energy level located in the band gap compared to that of the 560 nm luminescence.

The different variations in the two emission peaks with increasing temperature may be explained as follows. The 470 nm peak is more sensitive to temperature, as indicated by a four-fold decrease as the temperature increases from 10 to 100 K. This piece of information suggests that the 470 nm peak is related to a shallow energy level which is not thermally stable for electrons at this level. At temperatures lower than 100 K, most of the excited electrons return to the shallow level via non-radiative transition, which then leads to the 470 nm PL enhancement. However, as the temperature increases to above 100 K, most electrons in the shallow level are thermally ionized by taking a transition to the conduction band and may recombine through non-radiative transitions, resulting in the rapid decrease in the luminescence intensity at 470 nm. In comparison, the emission peak of 560 nm exhibits a smaller dependence on the temperature, suggesting that most of the electrons excited into the deeper defect energy level, which are thermally stable, will return to the ground state via radiative transitions. The intensity reduction with increasing temperature may thus be mainly induced by enhanced non-radiative recombination. Both the Gaussian-fitted emission peaks show a small red shift with increasing temperature, and it may be due to some variations in the band gaps at different temperatures [27].

Figure 5 shows the low-temperature PL spectra of sample B (SnO₂ nanobelts). The PL spectra show a temperature relationship similar to sample A, but the position of the luminescence peak is different. Both the first emission peak at 476 nm and second emission peak at 595 nm show a smaller red shift compared to sample A. These differences may be caused by the different band gaps between nanowires and nanobelts due to the different morphologies and sizes. Compared to sample A, the PL intensity from sample B is higher by about four times. In our study, the laser-irradiated area is the same and the nanostructure densities are consequently about the same. Thus, the big difference in the luminescence intensities from the nanowires and nanobelts may stem from the different morphologies because nanobelts have a larger surface area ratio than nanowires. The two emission peaks may also be related to defect states on the surface of the SnO₂ nanowires or nanobelts.

The semiconducting behaviour of tin oxide is attributed to the presence of oxygen vacancies, which is also crucial to their optical properties. Similar luminescence characteristics have been observed in SnO₂ powders and films at room temperature, and the origin of the luminescence is attributed to oxygen vacancies [26, 28]. Therefore, the observed photoluminescence in our experiments is probably related to defect energy levels originating from oxygen vacancies in the band gap of the SnO₂ nanowires or nanobelts. It has been suggested that the defect electronic states in the SnO₂ band gap can be associated with the surface rather than subsurface oxygen vacancies [29]. It should be noted that we still

cannot confirm unambiguously that the observed luminescence originates from surface oxygen vacancies, although our experimental results have provided some indirect evidence. More work is being conducted to identify the two different luminescence centres.

4. Summary

In summary, SnO₂ nanowires and nanobelts have been synthesized by thermal evaporation of Sn powders in the presence of oxygen. The morphology of the products depends on the reaction temperature. The microstructures and surface compositions of the nanowhiskers were characterized. Both the nanowires and nanobelts show two distinct emission peaks which depend strongly on the temperature. The luminescence mechanism is discussed and the surface oxygen vacancies are proposed to be the possible origin of the luminescence.

Acknowledgments

This work was financially supported by City University of Hong Kong Direct Allocation Grant No. 9360110, Science & Technology Committee of Shanghai (No. 0359nm204, 0252nm084, and 04JC14080), as well as the National Science Foundation of China, Grant No. 1022541.

References

- [1] Liu Y, Zheng C, Wang W, Yin C and Wang G 2001 *Adv. Mater.* **13** 1883
- [2] Dai Z R, Gole J L, Stout J D and Wang Z L 2002 *J. Phys. Chem. B* **106** 1274
- [3] Cheng B, Russell J M, Shi W S, Zhang L and Samulski E T 2004 *J. Am. Chem. Soc.* **126** 5972
- [4] Duan J H, Yang S G, Liu H W, Gong J F, Huang H B, Zhao X N, Zhang R and Du Y W 2005 *J. Am. Chem. Soc.* **127** 6180
- [5] Paraguay-Delgado F, Antunez-Flores W, Miki-Yoshida M, Aguilar-Elguezaba A, Santiago P, Diaz R and Ascencio J A 2005 *Nanotechnology* **16** 688
- [6] Kolmakov A, Klenov D O, Lilach Y, Stemmer S and Moskovits M 2005 *Nano Lett.* **5** 667
- [7] Liu Z Q, Zhang D H, Han S, Li C, Tang T, Jin W, Liu X L, Lei B and Zhou C W 2003 *Adv. Mater.* **15** 1754
- [8] Wang Y L, Jiang X C and Xia Y N 2003 *J. Am. Chem. Soc.* **125** 16176
- [9] Huang H, Tan O K, Lee Y C, Tran T D, Tse M S and Yao X 2005 *Appl. Phys. Lett.* **87** 163123
- [10] Comini E, Faglia G, Sberveglieri G, Pan Z and Wang Z L 2002 *Appl. Phys. Lett.* **81** 1869
- [11] Arnold M S, Avouris P, Pan Z W and Wang Z L 2003 *J. Phys. Chem. B* **107** 659
- [12] Kolmakov A, Zhang Y, Cheng G and Moskovits M 2003 *Adv. Mater.* **15** 997
- [13] Kalinin S V, Shin J, Jesse S, Geohegan D, Baddorf A P, Lilach Y, Moskovits M and Kolmakov A 2005 *J. Appl. Phys.* **98** 044503
- [14] Li Q H, Chen Y J, Wan Q and Wang T H 2004 *Appl. Phys. Lett.* **85** 1805
- [15] Hu J Q, Ma X L, Shang N G, Xie Z Y, Wong N B, Lee C S and Lee S T 2002 *J. Phys. Chem. B* **106** 3823
- [16] Hu J Q, Bando Y, Liu Q L and Golberg D 2003 *Adv. Funct. Mater.* **13** 493
- [17] Calestani D, Lazzarini L, Salviati G and Zha M 2005 *Cryst. Res. Technol.* **40** 937
- [18] Faglia G, Baratto C, Sberveglieri G, Zha M and Zappettini A 2005 *Appl. Phys. Lett.* **86** 011923

- [19] Cai D, Su Y, Chen Y, Jiang J, He Z and Chen L 2005 *Mater. Lett.* **59** 1984
- [20] Maestre D, Cremades A and Piqueras J 2005 *J. Appl. Phys.* **97** 044316
- [21] Wagner R S and Ellis W C 1964 *Appl. Phys. Lett.* **4** 89
- [22] Frohlich D and Kenkly R 1978 *Phys. Rev. Lett.* **41** 1750
- [23] Mills G, Li Z G and Meisel D 1988 *J. Phys. Chem.* **92** 822
- [24] Efros A L 1982 *Sov. Phys.—Semicond.* **16** 772
- [25] Brus L 1983 *J. Chem. Phys.* **79** 5566
- [26] Chang S S and Park D K 2002 *Mater. Sci. Eng. B* **95** 55
- [27] Varshni Y P 1967 *Physica* **34** 149
- [28] Jeong J, Choi S P, Chang C I, Shin D C, Park J S, Lee B T, Park Y J and Song H J 2003 *Solid State Commun.* **127** 595
- [29] Cox D F, Fryberger T B and Semancik S 1988 *Phys. Rev. B* **38** 2072